Poisson Coordinates

Xian-Ying Li and Shi-Min Hu, *Member*, *IEEE*

Abstract—Harmonic functions are the critical points of a Dirichlet energy functional, the linear projections of conformal maps. They play an important role in computer graphics, particularly for gradient-domain image processing and shape-preserving geometric computation. We propose Poisson coordinates, a novel transfinite interpolation scheme based on the Poisson integral formula, as a rapid way to estimate a harmonic function on a certain domain with desired boundary values. Poisson coordinates are an extension of the Mean Value coordinates (MVCs) which inherit their linear precision, smoothness, and kernel positivity. We give explicit formulas for Poisson coordinates in both continuous and 2D discrete forms. Superior to MVCs, Poisson coordinates are proved to be pseudoharmonic (i.e., they reproduce harmonic functions on n-dimensional balls). Our experimental results show that Poisson coordinates have lower Dirichlet energies than MVCs on a number of typical 2D domains (particularly convex domains). As well as presenting a formula, our approach provides useful insights for further studies on coordinates-based interpolation and fast estimation of harmonic functions.

Index Terms—Poisson integral formula, transfinite interpolation, barycentric coordinates, pseudoharmonic

✦

1 INTRODUCTION

H ARMONIC functions are continuous maps from an open subset of $\mathbb{R}^n$ and its boundary, $\Omega \bigcup \partial\Omega$, to $\mathbb{R}$; they are twice continuously differentiable in Ω and satisfy the Laplace's equation:

$$\Delta u = \frac{\partial^2 u}{\partial x_1^2} + \frac{\partial^2 u}{\partial x_2^2} + \cdots + \frac{\partial^2 u}{\partial x_n^2} = 0.$$

From a variational perspective, harmonic functions are the critical points of the following Dirichlet energy functional, which has been frequently used in *gradient-domain image processing* [1], [2], [3]:

$$E_D[w] = \frac{1}{2} \int_\Omega |\nabla w|^2 dx,$$

where ∇w is the gradient vector field of w.

Harmonic functions are also closely related to *conformal geometry* [4], [5], and play an important role in *shape-preserving geometric computation*, e.g., *surface parameterization* [6], [7], *space deformation* [8], [9], and *quadrilateral remeshing* [10].

In practice, we often face the problem to determine a harmonic function on a certain domain under conditions of fixed, continuous boundary values. This is known as the Dirichlet problem [11], and was well studied in the early 20th century. The existence and uniqueness of the solution as long as the domain's boundary contains no irregular point were proved by Hilbert [12] and Perron [13]. Furthermore, the solution to the Dirichlet problem is known to be a linear combination of boundary values in the following integral form:

$$u(x) = \int_{\zeta \in \partial\Omega} \mathcal{H}_\Omega(x,\zeta) f(\zeta) d\sigma(\zeta), \qquad (1)$$

where $d\sigma(\zeta)$ is the area element of $\partial\Omega$ at the boundary point ζ, and $f(\zeta)$ are the given boundary values, and $\mathcal{H}_\Omega(x,\zeta)$ are called the *harmonic coordinates* of x (in continuous form) with respect to each boundary point ζ. These harmonic coordinates are also closely related to Green's functions (refer to [14]).

To study the Dirichlet problem in the discrete case, we pay attention to simplicial polytopes (i.e., the polytopes whose facets are all simplices). For such polytopes, values are given at vertices, and all other boundary values are interpolated linearly within each facet. In such a case, (1) can be rewritten as

$$u(x) = \sum_{v \in V(P)} \mathcal{H}_P(x,v) f(v), \qquad (2)$$

where $V(P)$ are the vertices of polytope P, and $\mathcal{H}_P(x,v)$ are the harmonic coordinates of x (in discrete form) with respect to each vertex v. Readers may refer to DeRose et al. [15], [16] for further details on discrete harmonic coordinates.

Harmonic coordinates are uniquely determined by the domain Ω (or P in discrete case), but generally they do not have a closed-form expression except for a few specialized domains (e.g., n-dimensional balls). This inspires a number of numerical solvers to the Dirichlet problem [15], [16], [17], [18]. Both of them require to solve large sparse linear equations on certain global structures of the whole interior region.

As well as numerical methods, coordinates-based approaches have been proposed for fast transfinite interpolation. These techniques provide explicit expressions of harmonic-like functions with desired boundary values. As a representative instance, Floater's *Mean Value coordinates (MVCs)* [19], [20], [21], [22], [23] always produce smooth interpolations in both continuous and discrete cases. However, a crucial problem of MVCs is that they do not produce rigorous harmonic functions on the most ordinary regions: n-dimensional balls.

● *The authors are with Tsinghua National Laboratory for Information Science and Technology, Department of Computer Science and Technology, Tsinghua University, FIT Building, Beijing 100084, P.R. China.*
E-mail: lee.xianying@gmail.com, shimin@tsinghua.edu.cn.

In this work, we propose *Poisson coordinates*, an extension of MVCs. By allowing the projection spheres of MVCs to be translated and using the Poisson integral formula instead of the Circumferential Mean Value Theorem, we derive Poisson coordinates in continuous form, as a novel transfinite interpolation scheme. We then prove that Poisson coordinates are barycentric and also possess the same smoothness and kernel positivity as MVCs. Moreover, by choosing the projection spheres adaptively according to the positions of target points, Poisson coordinates are able to reproduce harmonic functions on n-dimensional balls. This important characteristic is called the *pseudoharmonic property* (see [24]). MVCs do not have this feature. Finally, we give an explicit formula for discrete Poisson coordinates on 2D polygons. Experimental results reveal that Poisson coordinates have lower Dirichlet energies than MVCs on a number of typical 2D domains, particularly convex domains.

1.1 Contributions

To the best of our knowledge, Poisson coordinates are the first transfinite interpolation technique to satisfy all of the following key properties:

- Poisson coordinates are explicit coordinates in both continuous case and 2D discrete case.
- Poisson coordinates inherit MVCs' linear precision, smoothness, and kernel positivity.
- Poisson coordinates are pseudoharmonic.

1.2 Overview

In Section 2, we will first review the coordinates-based transfinite interpolation methods. In Section 3, we will introduce the Poisson integral formula and then use it to derive the Poisson coordinates in continuous form. In Section 4, we will further present an explicit formula for discrete Poisson coordinates on 2D polygons. Experimental results will be displayed in Section 5.

2 BACKGROUND AND PREVIOUS WORK

Previous work on coordinates-based transfinite interpolation is copious. Here, we briefly review the best known approaches, with the emphasis on MVCs. Readers may refer to Belyaev's survey [24] for a detailed analysis of these coordinates in continuous form. For the discrete case, Ju et al. [25] provided an in-depth geometric explanation for general barycentric coordinates on convex simplicial polytopes.

2.1 Mean Value Transfinite Interpolation

MVCs were first established by Floater [19], where both an interpolation formula and the corresponding explicit discrete coordinates on 2D polygons were presented.

To estimate the value at an arbitrary point x within the kernel of Ω, a unit sphere S_x with center at x (the *projection sphere*) is constructed. For each point ξ on S_x, the ray $[x, \xi]$ crosses $\partial\Omega$ at a unique point ζ, as shown in Fig. 1.

We use $u(x)$ and $f(\zeta)$ to linearly estimate the value at the point ξ, denoted by $u_x(\xi)$

$$u_x(\xi) = u(x) + \frac{|x - \xi|}{|x - \zeta|}[f(\zeta) - u(x)], \quad (3)$$
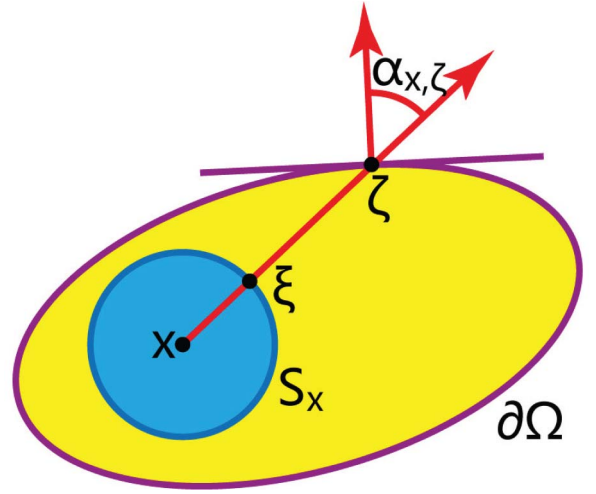
where $|x - \xi|$ is always equal to 1.

Fig. 1. MVCs computation: S_x is a unit sphere. ξ is on S_x. ζ is on $\partial\Omega$. $\alpha_{x,\zeta}$ is the intersection angle between the ray $[x, \zeta]$ and the outward normal of $\partial\Omega$ at ζ.

Inspired by the Circumferential Mean Value Theorem [14] of harmonic functions, MVCs require values in (3) to satisfy the following equation:

$$u(x) = \frac{1}{\omega_{n-1}} \int_{\xi \in S_x} u_x(\xi) d\sigma(\xi), \quad (4)$$

where ω_{n-1} is the surface area of a unit sphere in $\mathbb{R}^n$.

Substituting $u_x(\xi)$ in (4) with (3), we obtain Mean Value interpolation:

$$u(x) = \frac{1}{\Phi_\Omega(x)} \int_{\xi \in S_x} \frac{f(\zeta)}{|x - \zeta|} d\sigma(\xi), \quad (5)$$

where

$$\Phi_\Omega(x) = \int_{\xi \in S_x} \frac{1}{|x - \zeta|} d\sigma(\xi)$$

is a positive factor depending on Ω and x.

Note that there is a relation between the following $(n-1)$-dimensional area elements:

$$d\sigma(\xi) = \frac{\cos \alpha_{x,\zeta}}{|x - \zeta|^{n-1}} d\sigma(\zeta),$$

where $\alpha_{x,\zeta}$ is the intersection angle between the ray $[x, \zeta]$ and the outward normal of Ω at ζ. Therefore, (5) can be rewritten as

$$u(x) = \frac{1}{\Phi_\Omega(x)} \int_{\zeta \in \partial\Omega} \frac{\cos \alpha_{x,\zeta}}{|x - \zeta|^n} f(\zeta) d\sigma(\zeta), \quad (6)$$

with the MVCs in continuous form

$$\mathcal{MV}_\Omega(x, \zeta) = \frac{1}{\Phi_\Omega(x)} \frac{\cos \alpha_{x,\zeta}}{|x - \zeta|^n}, \quad (7)$$

where

$$\Phi_\Omega(x) = \int_{\zeta \in \partial\Omega} \frac{\cos \alpha_{x,\zeta}}{|x - \zeta|^n} d\sigma(\zeta).$$

Hormann and Floater [22] noticed that, (6) can be extended to the whole interior region, but not limited to the kernel. In fact, for x in Ω but outside the kernel, $[x, \xi)$ may

have multiple intersections with $\partial\Omega$: $\zeta_j (j = 1, \ldots, n(x, \xi))$; $n(x, \xi)$ odd. In such a case, we can rewrite the Mean Value formula (4) as

$$u(x) = \frac{1}{\omega_{n-1}} \int_{\xi \in S_x} \left(\sum_{j=1}^{n(x,\xi)} (-1)^{j-1} u_x(\xi) \right) d\sigma(\xi). \qquad (8)$$

Substituting the term $u_x(\xi)$ in (8) with

$$u_x(\xi) = u(x) + \frac{1}{|x - \zeta_j|}[f(\zeta_j) - u(x)],$$

we obtain

$$u(x) = \frac{1}{\Phi_\Omega(x)} \int_{\xi \in S_x} \left(\sum_{j=1}^{n(x,\xi)} (-1)^{j-1} \frac{f(\zeta_j)}{|x - \zeta_j|} \right) d\sigma(\xi), \qquad (9)$$

where

$$\Phi_\Omega(x) = \int_{\xi \in S_x} \left(\sum_{j=1}^{n(x,\xi)} \frac{(-1)^{j-1}}{|x - \zeta_j|} \right) d\sigma(\xi).$$

By rewriting the right-hand side of (9) as an equivalent integral over $\partial\Omega$, we can also obtain the same formula as in (6). Therefore, (6) is a transfinite interpolation.

Properties of MVCs are further discussed in [22] and [23]; it has been proved that MVCs are barycentric and smooth in 2D. In higher dimensions, similar properties have also been considered in [26].

In the discrete case, Floater [19] provided an explicit expression for discrete MVCs on 2D polygons, by calculating the integral in (6) by parts. For higher dimensions, Ju et al. [20] and Floater et al. [21] independently formulated explicit discrete MVCs on 3D simplicial polyhedrons.

More recently, Lipman et al. [27] sought coordinates $MV(x, \zeta)$ which are zero for all ζ invisible from x, and called the results *positive MVCs (PMVCs)*. However, PMVCs lack C^1 continuity.

2.2 Wachspress-Warren Transfinite Interpolation

Wachspress [28] discovered a barycentric interpolation formula on 2D polygons with affine-invariant discrete coordinates. Later, a geometric expression in terms of angles was given by Meyer et al. [29]. More recently, Warren et al. [30], [31] extended these coordinates to higher dimensions, not only for polytopes but also for general domains as a transfinite interpolation. However, *Wachspress-Warren coordinates* do not possess the kernel positivity.

2.3 Laplace Transfinite Interpolation

Schaefer et al. [32] described the *Laplace transfinite interpolation*. They minimized the Dirichlet energy of the piecewise linear function (3) to estimate the value at arbitrary points within the kernel. The discrete form of Laplace transfinite interpolation corresponds exactly to the well-known *discrete harmonic coordinates* (or *cotangent weights*) [33], [34], [35], which are widely used in finite element analysis and discrete differential geometry.

2.4 Pseudoharmonic Transfinite Interpolation

A transfinite interpolation is called *pseudoharmonic* if it reproduces harmonic functions on n-dimensional balls.

Belyaev [24] showed that none of the above methods (i.e., the Mean Value, Wachspress-Warren, and Laplace transfinite interpolations) are pseudoharmonic. In contrast, *Shepard transfinite interpolation* [36] is known to be pseudoharmonic [37]. However, Shepard interpolation is not barycentric, which greatly limits its usability. Another pseudoharmonic, barycentric scheme is *Gordon-Wixom transfinite interpolation* [38], whose 2D discrete form was first derived by Belyaev [24]. However, computing 2D discrete Gordon-Wixom coordinates requires prior division of all the polygon's sides, which might greatly enlarge the polygon's degree, especially for nonconvex polygons. Furthermore, the explicit expression for 2D discrete Gordon-Wixom coordinates is complex: Belyaev notes they are "too lengthy to present" [24]. Recently, Manson et al. proposed the *positive Gordon-Wixom coordinates* [39] with explicit expression for both 2D polygons and B-splines. However, positive Gordon-Wixom coordinates are not pseudoharmonic.

2.5 Other Transfinite Interpolation Approaches

Several other coordinates-based transfinite interpolation techniques have also been proposed. *Maximum Entropy coordinates* [40] are always nonnegative and smooth, but an explicit expression is not available, and a numerical calculation is required. *Moving Least Square coordinates* [41] can handle nonclosed and self-intersecting polygons, and can reproduce polynomial functions to an arbitrary specified degree, but the computational cost is high. More importantly, neither of these methods is pseudoharmonic.

3 CONTINUOUS POISSON COORDINATES

To improve MVCs, we first introduce the Poisson integral formula (in Section 3.1). Based on this formula, we then present Poisson transfinite interpolation with Poisson coordinates in continuous form (in Sections 3.2 and 3.3). We prove that Poisson coordinates are barycentric and pseudoharmonic.

3.1 Poisson Integral Formula

Consider the ball B_r in $\mathbb{R}^n$ centered at the origin with radius to r. There is an analytic solution to the Dirichlet problem on B_r via the following Poisson integral formula (see [14]):

$$u(x) = \int_{\zeta \in \partial B_r} \frac{r^2 - |x|^2}{r\omega_{n-1}|x - \zeta|^n} f(\zeta) d\sigma(\zeta), \qquad (10)$$

where ω_{n-1} is the surface area of the unit sphere in $\mathbb{R}^n$. Note that the Circumferential Mean Value Theorem is the special case of (10) when x is at the center.

By comparison to (1), this Poisson integral formula gives a closed-form expression for continuous harmonic coordinates on B_r:

$$\mathcal{H}_{B_r}(x, \zeta) = \frac{r^2 - |x|^2}{r\omega_{n-1}|x - \zeta|^n}, \qquad (11)$$

which is also called the Poisson kernel.

From (7) and (11), we can deduce that

$$\mathcal{MV}_{B_r}(x, \zeta) = \Lambda_{B_r}(x) \cos \alpha_{x,\zeta} \mathcal{H}_{B_r}(x, \zeta), \qquad (12)$$
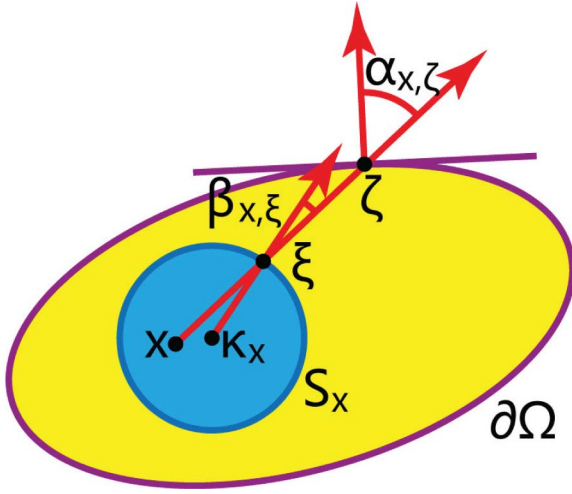
Fig. 2. Poisson coordinates computation: S_x is a translated unit sphere with center at κ_x. $\beta_{x,\xi}$ is the intersection angle between $[x, \xi]$ and $[\kappa_x, \xi]$.

where

$$\Lambda_{B_r}(x) = \frac{1}{\Phi_{B_r}(x)} \frac{r\omega_{n-1}}{r^2 - |x|^2}$$

is a positive factor relies on B_r and x.

From (12) we can easily see that

Proposition 1. *For $x \in B_r$, MVCs are equivalent to harmonic coordinates if and only if x is at the center.*

Proof. First, note that the coordinates $MV_{B_r}(x, \zeta)$ and $H_{B_r}(x, \zeta)$ are equivalent if and only if all the $\alpha_{x,\zeta}$ are the same. However, for the point ζ for which the ray $[x, \zeta)$ crosses the center, $\alpha_{x,\zeta}$ is exactly 0. Therefore, all the angles $\alpha_{x,\zeta}$ being the same means that they are all equal to 0, which implies that x is exactly at the center of B_r. □

This proposition reveals that MVCs are not pseudoharmonic. However, we will show in the next section that they can be modified to be pseudoharmonic if the projection spheres are translated appropriately.

3.2 Poisson Transfinite Interpolation

To formulate Poisson transfinite interpolation, we follow the notation in Section 2. But unlike MVCs, the center of S_x is not required to be x any more, and we now denote it by κ_x, as shown in Fig. 2.

Like MVCs, we retain the linear estimation in (3), but replace the Mean Value formula (4) with the following equation from the Poisson integral formula [14]:

$$u(x) = \frac{1 - |x - \kappa_x|^2}{\omega_{n-1}} \int_{\xi \in S_x} \frac{1}{|x - \xi|^n} u_x(\xi) d\sigma(\xi). \quad (13)$$

Note that

$$u(x) = \frac{1 - |x - \kappa_x|^2}{\omega_{n-1}} \int_{\xi \in S_x} \frac{1}{|x - \xi|^n} u(x) d\sigma(\xi),$$

thus (13) can be rewritten as

$$\int_{\xi \in S_x} \frac{1}{|x - \xi|^n} (u_x(\xi) - u(x)) d\sigma(\xi) = 0. \quad (14)$$

Substituting the $u_x(\xi)$ in (14) with (3), we obtain the following *Poisson interpolation*:

$$u(x) = \frac{1}{\Psi_{\Omega,S_x}(x)} \int_{\xi \in S_x} \frac{f(\zeta)}{|x - \zeta||x - \xi|^{n-1}} d\sigma(\xi), \quad (15)$$

where

$$\Psi_{\Omega,S_x}(x) = \int_{\xi \in S_x} \frac{1}{|x - \zeta||x - \xi|^{n-1}} d\sigma(\xi)$$

is a positive factor relies on Ω, x, and S_x.

Going a step further, note that

$$d\sigma(\xi) = \frac{\cos \alpha_{x,\zeta}}{\cos \beta_{x,\xi}} \frac{|x - \xi|^{n-1}}{|x - \zeta|^{n-1}} d\sigma(\zeta),$$

where $\beta_{x,\xi}$ is the intersection angle between $[x, \xi]$ and $[\kappa_x, \xi]$, thus we can rewrite (15) as the following *Poisson transfinite interpolation* (it is also for x outside the kernel of Ω, like MVCs, as discussed in Section 2):

$$u(x) = \frac{1}{\Psi_{\Omega,S_x}(x)} \int_{\zeta \in \partial\Omega} \frac{\cos \alpha_{x,\zeta}}{\cos \beta_{x,\xi}} \frac{1}{|x - \zeta|^n} f(\zeta) d\sigma(\zeta), \quad (16)$$

with the *Poisson coordinates* in continuous form:

$$\mathcal{P}_{\Omega,S_x}(x, \zeta) = \frac{1}{\Psi_{\Omega,S_x}(x)} \frac{\cos \alpha_{x,\zeta}}{\cos \beta_{x,\xi}} \frac{1}{|x - \zeta|^n}, \quad (17)$$

where

$$\Psi_{\Omega,S_x}(x) = \int_{\zeta \in \partial\Omega} \frac{\cos \alpha_{x,\zeta}}{\cos \beta_{x,\xi}} \frac{1}{|x - \zeta|^n} d\sigma(\zeta).$$

Since $\beta_{x,\xi}$ and $\alpha_{x,\zeta}$ are all acute for x within the kernel of Ω, it follows that the Poisson coordinates in (17) have kernel positivity. However, like MVCs, Poisson coordinates may be negative for points outside the kernel.

Next, we prove that Poisson coordinates have linear precision (i.e., they are barycentric).

Proposition 2. *Poisson coordinates have linear precision.*

Proof. Assume f is a linear function defined over the whole of $\mathbb{R}^n$. We show that Poisson transfinite interpolation reproduces f. This assertion is based on two observations:

First, (15) is the unique solution to (3) and (13).

Second, let $u(x) = f(x)$ and $u_x(\xi) = f(\xi)$, we show that they precisely satisfy (3) and (13) at the same time. In fact, (3) is satisfied because f is linear on the ray $[x, \xi]$. Also, (13) is satisfied because f is harmonic, so Poisson integral formula reproduces f. It follows that $u(x) = f(x)$ is a solution to (3) and (13).

Therefore, (15) must be exactly equal to $f(x)$ due to the uniqueness of the solution, which implies Poisson coordinates have linear precision. □

3.3 Placement of Projection Spheres

Note that kernel positivity and linear precision of Poisson coordinates do not depend on the positions of projection spheres. However, these spheres surely affect the interpolation. In this section, we present a strategy to adaptively place the projection spheres (i.e., to place the centers κ_x), and then prove that Poisson coordinates are pseudoharmonic with this placement.
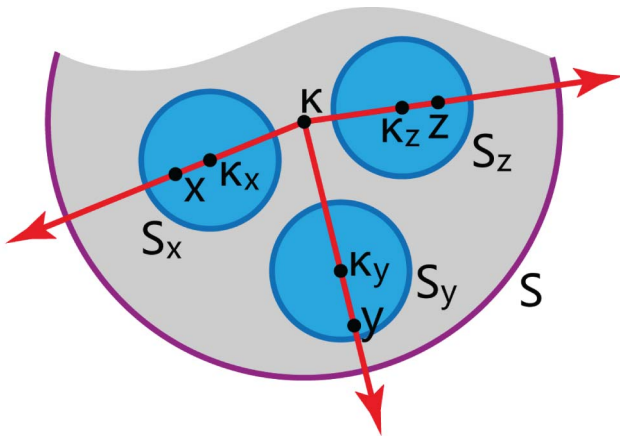
Fig. 3. Regular placement: S is the "base sphere" with center at κ and radius to r. S_x is a unit projection sphere, whose center κ_x lies on the ray $[x, \kappa]$ and satisfies $\kappa_x = x + (\kappa - x)/r$, so that S_x and S are homothetic, and x is their homothetic center. S_y and S_z are similar.

We first introduce the concept of *regular placement*.

Definition 1. *Let S be a sphere that covers Ω, a placement of the projection spheres is said to be regular with respect to S, if each projection sphere S_x is homothetic to S, with x be the homothetic center, i.e., the center κ_x satisfies*

$$\kappa_x = x + (\kappa - x)/r, \qquad (18)$$

as shown in Fig. 3. S is said to be the base sphere *of this regular placement.*

Regular placement is an important concept. With regular placement, the angle $\beta_{x,\xi}$ can be translated along $[x, \xi]$ to locate its vertex on the base sphere (see Fig. 4, where $\beta_{x,\xi} = \beta_{x,\eta}$). Since S is a fixed sphere, $\beta_{x,\xi}(= \beta_{x,\eta})$ is analytic, which guarantees the smoothness of Poisson coordinates.

Proposition 3. *With regular placement, Poisson coordinates in (17) are smooth (C^∞) in Ω.*

Proof. With regular placement, both of $\cos \alpha_{x,\zeta}$, $\cos \beta_{x,\xi}$, and $|x - \zeta|^n$ are analytic. Therefore, the Poisson coordinates in (17) are composed of analytic functions and thus are C^∞ in Ω.   □

More than the interior smoothness, regular placement also guarantees the continuity of the interpolation on the boundary $\partial\Omega$.

Proposition 4. *With regular placement, if the given boundary values f are continuous on $\partial\Omega$, and the Condition 1 in Appendix, which can be found on the Computer Society Digital Library at http://doi.ieeecomputersociety.org/10.1109/TVCG.2012.109, is satisfied, then the function u in (16) converges to f at the boundary $\partial\Omega$ (i.e., u interpolates f).*

Proof of Proposition 4 can be found in the Appendix, available in the online supplemental material, and readers may skip it without loss of continuity.

By choosing different base spheres, there is a family of regular placements. However, we next focus on the following unique *basic regular placement*.
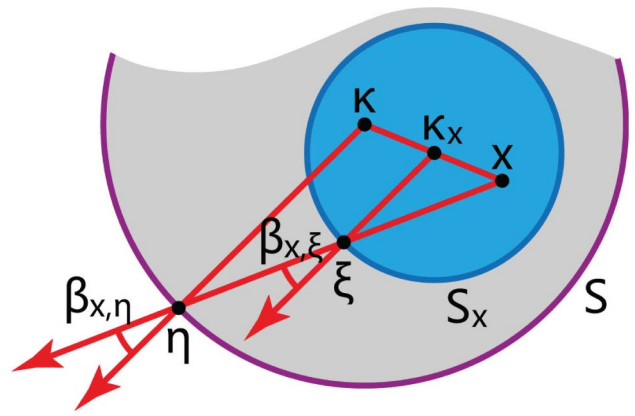

Fig. 4. Translate the angle $\beta_{x,\xi}$ along $[x, \xi]$ to locate its vertex on the base sphere. Note that $\beta_{x,\xi} = \beta_{x,\eta}$, due to the homothety.

Definition 2. *Let S_Ω be the smallest sphere that covers Ω. The regular placement with respect to S_Ω is said to be the basic regular placement.*

We prove that Poisson coordinates using the basic regular placement are pseudoharmonic.

Proposition 5. *With basic regular placement, Poisson coordinates are pseudoharmonic.*

Proof. Let Ω be the n-dimensional ball B_r. With basic regular placement, S_{B_r} is B_r itself, so in this case, we have $\alpha_{x,\zeta} = \beta_{x,\eta} = \beta_{x,\xi}$. Thus, the Poisson coordinates in (17) can be rewritten as the Poisson kernel in (11) multiplied by a positive factor. Hence, they are equivalent, which implies that Poisson coordinates are pseudoharmonic.   □

So far, we have shown that Poisson coordinates possess kernel positivity and linear precision, and, using basic regular placement of projection spheres, they are pseudoharmonic and smooth. In the next section, we will consider the discrete case and give an explicit formula for discrete Poisson coordinates on 2D polygons.

4   DISCRETE POISSON COORDINATES

Suppose P is a simplicial polytope in $\mathbb{R}^n$, with vertices $v_1, v_2, \ldots, v_m$ and facets $F_1, F_2, \ldots, F_h$. To formulate discrete Poisson coordinates on P, we divide the integral in (15) into parts by facets

$$I(F_j) = \delta_{F_j} \int_{\xi \in S_{F_j}, \zeta \in F_j} \frac{f(\zeta)}{|x - \zeta| \|x - \xi\|^{n-1}} d\sigma(\xi), \qquad (19)$$

where δ_{F_j} is a sign that depends on x and F_j. δ_{F_j} equals 1 if x lies on the opposite side of F_j's plane with respect to F_j's outward normal; otherwise, δ_{F_j} equals -1. S_{F_j} is the intersection of S_x and the interior of pyramid $x - F_j$ (for an example of S_{F_j}, see the red arc in Fig. 5).

Note that $I(F_j)$ is exactly 0 if x lies in the plane that contains F_j, so we will focus on the case that x is not coplanar with F_j. Suppose the boundary values $f(\zeta)$ are linear interpolated in the simplex facet F_j, which can be written as
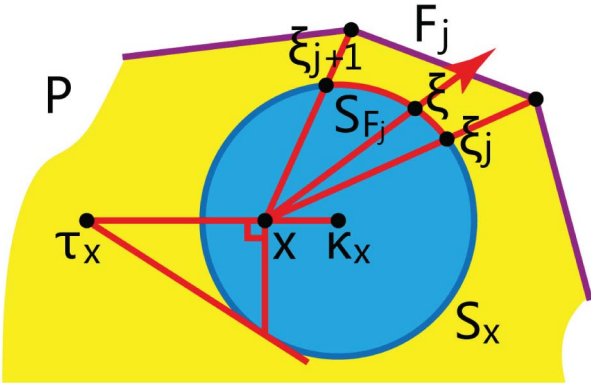
Fig. 5. 2D discrete Poisson coordinates: F_j is the target facet (side). τ_x is the inverse of x with respect to S_x.

$$f(\zeta) = \sum_{k:v_k \in F_j} (\zeta - x) \cdot \frac{\mu_{F_j,v_k}}{(v_k - x) \cdot \mu_{F_j,v_k}} f(v_k), \qquad (20)$$

where $\cdot$ denotes the inner product of vectors; μ_{F_j,v_k} is a normal vector to the lateral facet of pyramid $x - F_j$ opposite vertex v_k.

Substituting (20) into (19), we obtain

$$I(F_j) = \sum_{k:v_k \in F_j} \Upsilon_{F_j} \cdot \omega_{F_j,v_k} f(v_k), \qquad (21)$$

where

$$\Upsilon_{F_j} = \int_{\xi \in S_{F_j}} \frac{\xi - x}{|\xi - x|^n} d\sigma(\xi) \qquad (22)$$

is an n-dimensional vector for each facet F_j, and

$$\omega_{F_j,v_k} = \begin{cases} 0 & \text{if } x \text{ is coplanar with } F_j, \\ \delta_{F_j} \dfrac{\mu_{F_j,v_k}}{(v_k - x) \cdot \mu_{F_j,v_k}} & \text{otherwise.} \end{cases} \qquad (23)$$

Substituting (21) into (15), we rewrite Poisson transfinite interpolation as

$$u(x) = \frac{\sum_{k=1}^m f(v_k) \sum_{j:v_k \in F_j} \Upsilon_{F_j} \cdot \omega_{F_j,v_k}}{\sum_{k=1}^m \sum_{j:v_k \in F_j} \Upsilon_{F_j} \cdot \omega_{F_j,v_k}}, \qquad (24)$$

with *discrete Poisson coordinates*

$$\mathcal{P}_{P,S_x}(x, v_k) = \frac{\sum_{j:v_k \in F_j} \Upsilon_{F_j} \cdot \omega_{F_j,v_k}}{\sum_{l=1}^m \sum_{j:v_l \in F_j} \Upsilon_{F_j} \cdot \omega_{F_j,v_l}}. \qquad (25)$$

The greatest challenge to computing discrete Poisson coordinates in (25) is to calculate Υ_{F_j}. We will next give a closed-form expression for Υ_{F_j} for the case of $n = 2$. What is more, for 2D polygons, each vertex v_k has exactly two neighboring facets (sides) F_j ($v_k \in F_j$), thus the discrete Poisson coordinates are in closed form before normalization (i.e., the numerators in (25) are), as for MVCs.

4.1 Discrete Poisson Coordinates on 2D Polygons

For $n = 2$, we denote the arc S_{F_j} by $\widehat{\xi_j \xi_{j+1}}$ (we may as well suppose it is in counterclockwise).

We next provide a closed-form expression for Υ_{F_j}. To easy calculate the integral on the right-hand side of (22), we move to the complex plane and endue each symbol with the meaning of its corresponding complex number

(i.e., each 2D vector (a, b) is interpreted as a complex number $a + ib$). We can now show that

Proposition 6. *For $n = 2$, Υ_{F_j} in (22) can be written as*

$$\Upsilon_{F_j} = \begin{cases} i(\xi_j - \xi_{j+1}) & \text{if } x = \kappa_x, \\ i(\tau_x - \kappa_x)\text{Log } \dfrac{\xi_{j+1} - \tau_x}{\xi_j - \tau_x} & \text{if } x \neq \kappa_x, \end{cases} \qquad (26)$$

where i is the imaginary unit; $\tau_x = \kappa_x + (x - \kappa_x)/|x - \kappa_x|^2$ is the inverse of x with respect to the circle S_x, as shown in Fig. 5. The logarithm function is $\text{Log } z = \ln|z| + i\text{Arg } z$ with principle argument $\text{Arg } z \in (-\pi, \pi]$.

Proof. Note that (26) is translation invariant (i.e., it is unchanged by adding a constant to all variables). Thus, we may as well suppose that $\kappa_x = 0$.

Using

$$d\sigma(\xi) = \frac{d\xi}{i\xi} \text{ and } \frac{\xi - x}{|\xi - x|^2} = \frac{1}{1/\xi - \overline{x}},$$

where $\overline{x}$ is the conjugate complex of x, we can write Υ_{F_j} in (22) as the following complex integral:

$$\Upsilon_{F_j} = -i \int_{\xi_j}^{\xi_{j+1}} \frac{1}{1 - \overline{x}\xi} d\xi. \qquad (27)$$

Clearly, (27) is equal to $i(\xi_j - \xi_{j+1})$ when $x = 0$. For $x \neq 0$, (27) is equal to

$$\Upsilon_{F_j} = i\tau_x \int_{\xi_j}^{\xi_{j+1}} \frac{1}{\xi - \tau_x} d\xi, \qquad (28)$$

where $\tau_x = 1/\overline{x}$ is the inverse of x with respect to S_x. Note that τ_x is outside the circle S_x; therefore, the winding number of S_x around τ_x is exactly zero, and hence the integral

$$\int_{\xi_j}^{\xi_{j+1}} \frac{1}{\xi - \tau_x} d\xi$$

in (28) equals $\text{Log } \dfrac{\xi_{j+1} - \tau_x}{\xi_j - \tau_x}$, completing the proof of Proposition 6. $\qquad \square$

After presenting the closed-form expression for Υ_{F_j}, we next calculate the 2D discrete Poisson coordinates. We first rewrite the numerators of (25) as

$$\mathcal{P}_{P,S_x}^{\sim}(x, v_j) = \Upsilon_{F_j} \cdot \omega_{F_j,v_j} + \Upsilon_{F_{j-1}} \cdot \omega_{F_{j-1},v_j}, \qquad (29)$$

where F_j is the side $[v_j, v_{j+1}]$, and all the indices are interpreted modulo m (i.e., $v_0 = v_m$ and $v_{m+1} = v_1$). $\mathcal{P}_{P,S_x}^{\sim}(x, v_j)$ are called the *unnormalized discrete Poisson coordinates*. From them, discrete Poisson coordinates can be obtained via

$$\mathcal{P}_{P,S_x}(x, v_j) = \mathcal{P}_{P,S_x}^{\sim}(x, v_j) \bigg/ \sum_k \mathcal{P}_{P,S_x}^{\sim}(x, v_k). \qquad (30)$$

Now, let us consider the term $\Upsilon_{F_j} \cdot \omega_{F_j,v_j}$ in (29). Note that ω_{F_j,v_j} equals 0 if x is colinear with side $[v_j, v_{j+1}]$, which implies $\Upsilon_{F_j} \cdot \omega_{F_j,v_j}$ is also equal to 0. So, we next assume that x is not colinear with $[v_j, v_{j+1}]$. Using (23), we can have
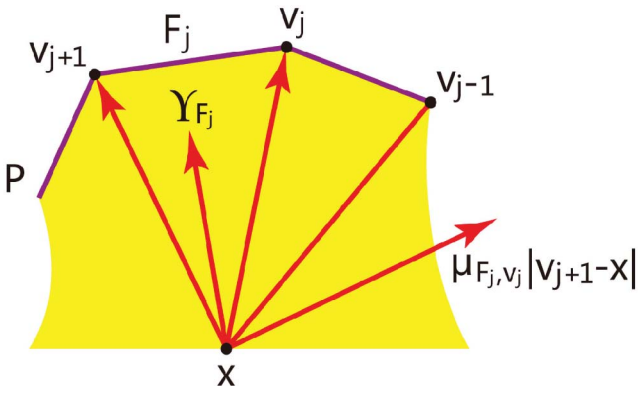
Fig. 6. 2D discrete Poisson coordinates: $\mu_{F_j,v_j}|v_{j+1}-x|$ is a vector obtained by rotating $\overrightarrow{xv_{j+1}}$ 90 degrees toward the side that $\overrightarrow{xv_j}$ lies in.

$$\Upsilon_{F_j} \cdot \omega_{F_j,v_j} = \delta_{F_j} \frac{\Upsilon_{F_j} \cdot \mu_{F_j,v_j}}{(v_j - x) \cdot \mu_{F_j,v_j}}$$
$$= \frac{\Upsilon_{F_j} \cdot (\mu_{F_j,v_j}|v_{j+1}-x|)}{\delta_{F_j}(v_j - x) \cdot (\mu_{F_j,v_j}|v_{j+1}-x|)}.$$

Note that $\mu_{F_j,v_j}|v_{j+1}-x|$ is a vector obtained by rotating $\overrightarrow{xv_{j+1}}$ 90 degrees toward the side that $\overrightarrow{xv_j}$ lies in (see Fig. 6). Thus, we have

$$\Upsilon_{F_j} \cdot (\mu_{F_j,v_j}|v_{j+1}-x|) = |\Upsilon_{F_j} \times (v_{j+1}-x)|,$$

where $\times$ denotes the cross product of vectors, and

$$\delta_{F_j}(v_j - x) \cdot (\mu_{F_j,v_j}|v_{j+1}-x|) = 2A_{\triangle xv_jv_{j+1}},$$

where $A_{\triangle XYZ}$ denotes the signed area of triangle XYZ. Therefore, the unnormalized 2D discrete Poisson coordinates in (29) can be rewritten as follow (suppose that x is not colinear with side $[v_{j-1}, v_j]$ either):

$$\mathcal{P}^{\sim}_{P,S_x}(x,v_j) = \frac{|\Upsilon_{F_j} \times (v_{j+1}-x)|}{2A_{\triangle xv_jv_{j+1}}} + \frac{|\Upsilon_{F_{j-1}} \times (v_{j-1}-x)|}{2A_{\triangle xv_{j-1}v_j}}. \quad (31)$$

Note that when $x = \kappa_x$, the vector $\Upsilon_{F_j} = i(\xi_j - \xi_{j+1})$ lies along the bisector of $\angle v_j x v_{j+1}$, and its length equals $|\xi_j - \xi_{j+1}| = 2\sin(\angle v_j x v_{j+1}/2)$. In this case, we have

$$\frac{|\Upsilon_{F_j} \times (v_{j+1}-x)|}{2A_{\triangle v_jxv_{j+1}}} = \frac{2|v_{j+1}-x|\sin^2(\angle v_j x v_{j+1}/2)}{|v_{j+1}-x||v_j-x|\sin \angle v_j x v_{j+1}}$$
$$= \frac{1}{|v_j - x|} \tan \frac{\angle v_j x v_{j+1}}{2},$$

and hence (31) can be rewritten as

$$\mathcal{P}^{\sim}_{P,S_x}(x,v_j) = \frac{1}{|v_j - x|}\left(\tan \frac{\angle v_j x v_{j+1}}{2} + \tan \frac{\angle v_{j-1} x v_j}{2}\right),$$

which corresponds exactly to MVCs.

Pseudocode for 2D discrete Poisson coordinates computation is summarized in Algorithm 1.

Algorithm 1. 2D discrete Poisson coordinates
Input : polygon $P = \{v_1, v_2, \ldots, v_m\}$, target point x inside P, and projection sphere S_x.
Output: Poison coordinates $\mathcal{P}_j$ ($j = 1, 2, \ldots, m$).
Compute the intersections ξ_j between $[x, v_j]$ and S_x.
Compute the 2D vectors Υ_{F_j} using (26).
for j from 1 to m **do**

$\mathcal{P}^{\sim}_j \leftarrow 0$
if x is not colinear with $[v_j, v_{j+1}]$ **then**

$$\mathcal{P}^{\sim}_j \leftarrow \mathcal{P}^{\sim}_j + \frac{|\Upsilon_{F_j} \times (v_{j+1}-x)|}{2A_{\triangle xv_jv_{j+1}}}.$$

end if
if x is not colinear with $[v_{j-1}, v_j]$ **then**

$$\mathcal{P}^{\sim}_j \leftarrow \mathcal{P}^{\sim}_j + \frac{|\Upsilon_{F_{j-1}} \times (v_{j-1}-x)|}{2A_{\triangle xv_{j-1}v_j}}.$$

end if
end for
$S_{\mathcal{P}} \leftarrow \sum_k \mathcal{P}^{\sim}_k.$
for j from 1 to m **do**
$\mathcal{P}_j \leftarrow \mathcal{P}^{\sim}_j / S_{\mathcal{P}}.$
end for

5 RESULTS AND DISCUSSION

We demonstrate Poisson coordinates (with basic regular placement) on various 2D polygons in Fig. 7, and compare them to both discrete harmonic coordinates and MVCs. Note that both MVCs and Poisson coordinates are smooth. To illustrate that Poisson coordinates are closer to discrete harmonic coordinates than MVCs, we exhibit the Dirichlet energies of both Poisson coordinates and MVCs in Table 1, and further show their differences to discrete harmonic coordinates in the last two columns of Fig. 7.

Table 1 contains the Dirichlet energies of discrete harmonic coordinates (denoted by E_0), Poisson coordinates (denoted by E_1), and MVCs (denoted by E_2), for the polygons in Fig. 7. These energies are calculated using a numerical method with a $1,500 \times 1,500$ grid. To compare Poisson coordinates and MVCs, we then calculate the ratio of differences: $R = (E_1 - E_0)/(E_2 - E_0)$. If R is less than 1, this implies that Poisson coordinates have lower Dirichlet energy than MVCs. Note that for the disk-like polygon (b), R is quite small, because Poisson coordinates are pseudo-harmonic, but MVCs are not (see also Fig. 7b, where Poisson coordinates and discrete harmonic coordinates are almost the same, but MVCs are quite different). For the typical convex polygons (a) and (c), R is around 50 percent, while for the concave polygon (d), R is close to 1. This reveals that Poisson coordinates and MVCs have comparable Dirichlet energies for concave regions. From Fig. 7d, we can see that Poisson coordinates and MVCs may be negative for points outside the kernel of the domain (e.g., either of them are negative in the right side region of the yellow segment). Also, we can see from the contour lines that Poisson coordinates and MVCs behave analogously, but differently from discrete harmonic coordinates, for concave polygons.

Other than the good performance of harmonic approximation, another key feature of Poisson coordinates is that they allow users to define their own placements for projection spheres for different purposes. In this paper, we have described the regular placement, particularly the basic regular placement. Note that MVCs can also be considered to be Poisson coordinates with a regular placement, where the radius of the base sphere is infinity. The technique of PMVCs [27] could also be applied to Poisson coordinates, however
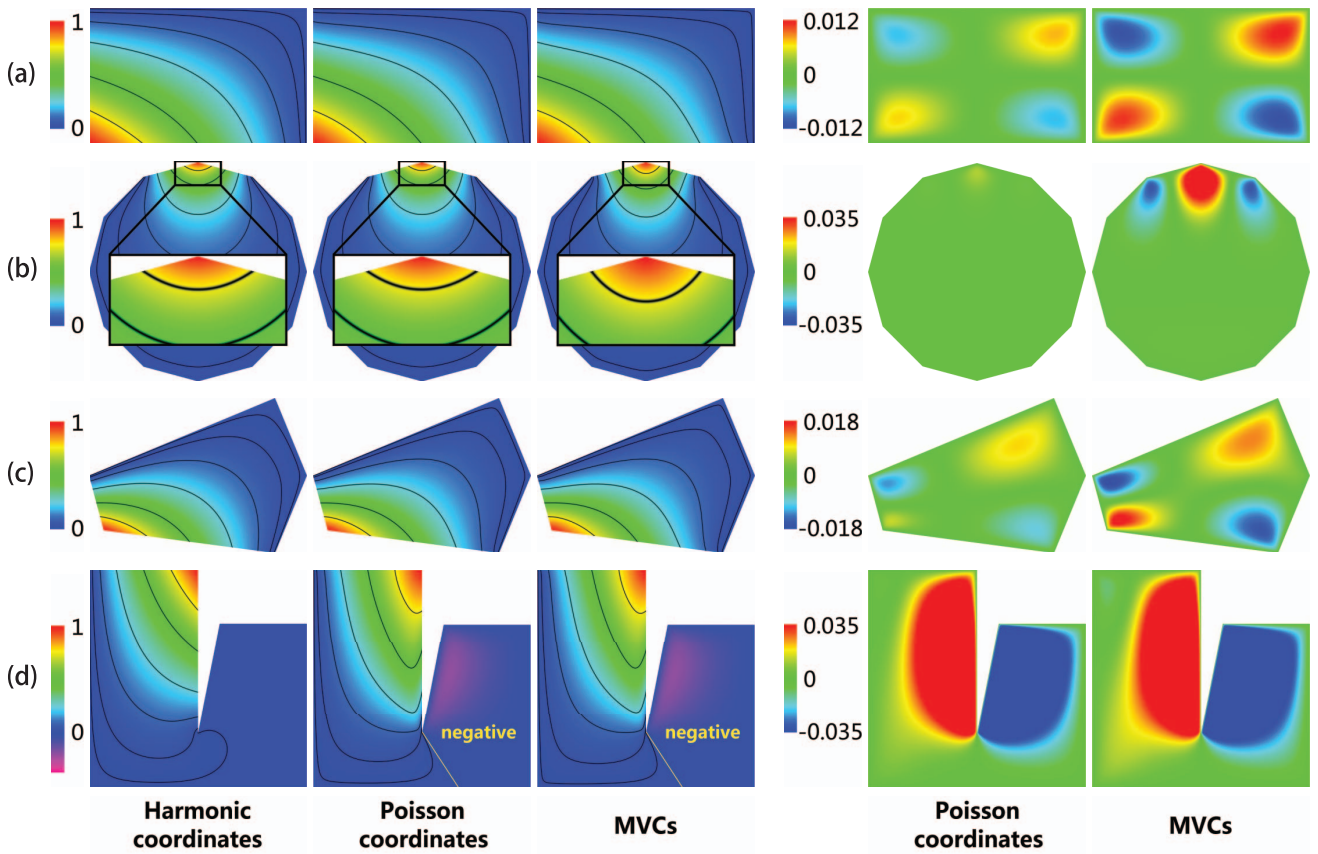
Fig. 7. The left three columns illustrate the results of discrete harmonic coordinates, Poisson coordinates (with basic regular placement), and MVCs for 2D polygons; contour lines for values $0.75, 0.50, 0.25, 0.10, 0.03, 0.005$ are in black. The right two columns show the DIFFERENCES between either Poisson coordinates or MVCs and discrete harmonic coordinates. Dirichlet energies of the left 12 subfigures are shown in Table 1.

that is beyond the scope of this paper. A weak point of our approach is that Poisson coordinates with a regular placement can only be extended to the interior region of the base sphere, but MVCs can be extended to the entire space, since their base sphere is infinite.

6 SUMMARY AND FUTURE WORK

In this paper, we introduced Poisson coordinates, and gave explicit formulas for Poisson coordinates in both continuous and 2D discrete cases. Poisson coordinates have MVCs' kernel positivity and linear precision, and allow placing the projection spheres at will. We further introduced the concept of regular placement, and particularly basic regular placement, using which the Poisson coordinates are smooth and pseudoharmonic. We also derived an explicit formula for discrete Poisson coordinates on 2D polygons. Experiments showed that Poisson coordinates are "more harmonic" than MVCs on a set of typical 2D convex polygons.

We believe this work will provide useful ideas for further studies on barycentric coordinates and transfinite interpolation. On the theoretical end, it would be useful to give an explicit formula for discrete Poisson coordinates in higher dimensions (i.e., to give an explicit formula for the Υ_{F_j} in (22) for $n \geq 3$). On the practical end, it is also possible to build alternative Poisson coordinates using different placement of the projection spheres, which may help provide desired boundary behaviors or overcome other restrictions.

Finally, the authors conjecture that

Conjecture 1. *With basic regular placement, Poisson coordinates always have lower Dirichlet energies than MVCs, for arbitrary 2D convex domains.*

TABLE 1
Dirichlet Energies for Fig. 7

	(a)	(b)	(c)	(d)
E_0 (Harmonic coordinates)	0.7459	0.8290	1.0319	0.7049
E_1 (Poisson coordinates)	0.7486	0.8312	1.0359	1.4025
E_2 (MVCs)	0.7507	0.8661	1.0414	1.4051
$R = (E_1 - E_0)/(E_2 - E_0)$	56.2%	0.59%	42.1%	99.6%

REFERENCES

[1] R. Fattal, D. Lischinski, and M. Werman, "Gradient Domain High Dynamic Range Compression," *ACM Trans. Graphics,* vol. 21, no. 3, pp. 249-256, 2002.
[2] P. Pérez, M. Gangnet, and A. Blake, "Poisson Image Editing," *ACM Trans. Graphics,* vol. 22, no. 3, pp. 313-318, 2003.

[3] A. Levin, A. Zomet, S. Peleg, and Y. Weiss, "Seamless Image Stitching in the Gradient Domain," *Proc. Eighth European Conf. Computer Vision (ECCV '04)*, pp. 377-389, 2004.

[4] X.D. Gu and S.T. Yau, *Computational Conformal Geometry*. Int'l Press, 2008.

[5] O. Weber and C. Gotsman, "Controllable Conformal Maps for Shape Deformation and Interpolation," *ACM Trans. Graphics*, vol. 29, no. 4, article 78, pp. 1-11, 2010.

[6] M.S. Floater and K. Hormann, "Surface Parameterization: A Tutorial and Survey," *Advances in Multiresolution for Geometric Modelling*, pp. 157-186, Springer, 2005.

[7] K. Hormann, B. Lévy, and A. Sheffer, "Mesh Parameterization: Theory and Practice," *Proc. SIGGRAPH Course Notes*, 2007.

[8] Y. Lipman, D. Levin, and D. Cohen-Or, "Green Coordinates," *ACM Trans. Graphics*, vol. 27, no. 3, article 78, pp. 1-10, 2008.

[9] M. Ben-Chen, O. Weber, and C. Gotsman, "Variational Harmonic Maps for Space Deformation," *ACM Trans. Graphics*, vol. 28, no. 3, article 34, pp. 1-11, 2009.

[10] S. Dong, S. Kircher, and M. Garland, "Harmonic Functions for Quadrilateral Remeshing of Arbitrary Manifolds," *Computer Aided Geometric Design*, vol. 22, no. 5, pp. 392-423, July 2005.

[11] L. Gårding, "The Dirichlet Problem," *The Math. Intelligencer*, vol. 2, no. 1, pp. 43-53, 1976.

[12] D. Hilbert, "Über Das Dirichletsche Prinzip," *Math. Annalen*, vol. 59, no. 1, pp. 161-186, 1904.

[13] O. Perron, "Eine Neue Behandlung Der Ersten Randwertaufgabe Für $\Delta u = 0$," *Math. Zeitschrift*, vol. 18, no. 1, pp. 42-54, 1923.

[14] N. Zeev, *Conformal Mapping*. Dover, 1952.

[15] T. DeRose and M. Meyer, "Harmonic Coordinates," technical report, Pixar Animation Studios, 2006.

[16] P. Joshi, M. Meyer, T. DeRose, B. Green, and T. Sanocki, "Harmonic Coordinates for Character Articulation," *ACM Trans. Graphics*, vol. 26, no. 3, article 71, pp. 1-9, 2007.

[17] D. Greenspan, "On the Numerical Solution of Dirichlet Problems," *The Quarterly J. Mechanics and Applied Math.*, vol. 12, no. 1, pp. 117-123, 1959.

[18] R.M. Rustamov, "Boundary Element Formulation of Harmonic Coordinates," technical report, Dept. of Math., Purdue Univ., 2008.

[19] M.S. Floater, "Mean Value Coordinates," *Computer Aided Geometric Design*, vol. 20, no. 1, pp. 19-27, Mar. 2003.

[20] T. Ju, S. Schaefer, and J. Warren, "Mean Value Coordinates for Closed Triangular Meshes," *ACM Trans. Graphics*, vol. 24, no. 3, pp. 561-566, 2005.

[21] M.S. Floater, G. Kós, and M. Reimers, "Mean Value Coordinates in 3D," *Computer Aided Geometric Design*, vol. 22, no. 7, pp. 623-631, Oct. 2005.

[22] K. Hormann and M.S. Floater, "Mean Value Coordinates for Arbitrary Planar Polygons," *ACM Trans. Graphics*, vol. 25, no. 4, pp. 1424-1441, 2006.

[23] C. Dyken and M.S. Floater, "Transfinite Mean Value Interpolation," *Computer Aided Geometric Design*, vol. 26, no. 1, pp. 117-134, Jan. 2009.

[24] A. Belyaev, "On Transfinite Barycentric Coordinates," *Proc. Fourth Eurographics Symp. Geometry Processing (SGP '06)*, pp. 89-99, 2006.

[25] T. Ju, P. Liepa, and J. Warren, "A General Geometric Construction of Coordinates in a Convex Simplicial Polytope," *Computer Aided Geometric Design*, vol. 24, no. 3, pp. 161-178, Apr. 2007.

[26] S. Bruvolla and M.S. Floater, "Transfinite Mean Value Interpolation in General Dimension," *J. Computational and Applied Math.*, vol. 233, no. 7, pp. 1631-1639, 2010.

[27] Y. Lipman, J. Kopf, D. Cohen-Or, and D. Levin, "Gpu-Assisted Positive Mean Value Coordinates for Mesh Deformations," *Proc. Fifth Eurographics Symp. Geometry Processing (SGP '07)*, pp. 117-123, 2007.

[28] E. Wachspress, *A Rational Finite Element Basis*. Academic Press, 1975.

[29] M. Meyer, H. Lee, A. Barr, and M. Desbrun, "Generalized Barycentric Coordinates on Irregular Polygons," *J. Graphics Tools*, vol. 7, no. 1, pp. 13-22, 2002.

[30] J. Warren, "Barycentric Coordinates for Convex Polytopes," *Advances in Computational Math.*, vol. 6, no. 1, pp. 97-108, 1996.

[31] J. Warren, S. Schaefer, A.N. Hirani, and M. Desbrun, "Barycentric Coordinates for Convex Sets," *Advances in Computational Math.*, vol. 27, no. 3, pp. 319-338, 2007.

[32] S. Schaefer, T. Ju, and J. Warren, "A Unified, Integral Construction for Coordinates over Closed Curves," *Computer Aided Geometric Design*, vol. 24, nos. 8/9, pp. 481-493, Nov. 2007.

[33] N.H. Christ, R. Friedberg, and T.D. Lee, "Weights of Links and Plaquettes in a Random Lattice," *Nuclear Physics B*, vol. 240, no. 3, pp. 337-346, 1982.

[34] U. Pinkall and K. Polthier, "Computing Discrete Minimal Surfaces and Their Conjugates," *Experimental Math.*, vol. 2, no. 1, pp. 15-36, 1993.

[35] M. Eck, T.D. DeRose, T. Duchamp, H. Hoppe, M. Lounsbery, and W. Stuetzle, "Multiresolution Analysis of Arbitrary Meshes," *Proc. SIGGRAPH '95*, pp. 173-182, 1995.

[36] D. Shepard, "A Two-Dimensional Interpolation Function for Irregularly-Spaced Data," *Proc. 23rd ACM Nat'l Conf.*, pp. 517-524, 1968.

[37] V. Caselles, J.M. Morel, and C. Sbert, "An Axiomatic Approach to Image Interpolation," *IEEE Trans. Image Processing*, vol. 7, no. 3, pp. 376-386, Mar. 1998.

[38] W.J. Gordon and J.A. Wixom, "Pseudo-Harmonic Interpolation on Convex Domains," *SIAM J. Numerical Analysis*, vol. 11, no. 5, pp. 909-933, Oct. 1974.

[39] J. Manson, K. Li, and S. Schaefer, "Positive Gordon-Wixom Coordinates," *Computer Aided Design*, vol. 43, no. 11, pp. 1422-1426, 2011.

[40] K. Hormann and N. Sukumar, "Maximum Entropy Coordinates for Arbitrary Polytopes," *Computer Graphics Forum*, vol. 27, no. 5, pp. 1513-1520, 2008.

[41] J. Manson and S. Schaefer, "Moving Least Squares Coordinates," *Proc. Symp. Geometry Processing*, pp. 1517-1524, 2010.

Xian-Ying Li received the bachelor's degree in computer science from Tsinghua University in 2008. He is currently working toward the PhD degree from Tsinghua University, Beijing. He received a gold medal of the International Mathematical Olympiad (IMO) in 2004 when he was 16 years old. His research interests include computer graphics, geometric modeling, and computational origami.

Shi-Min Hu received the PhD degree from Zhejiang University in 1996. He is currently a professor in the Department of Computer Science and Technology, Tsinghua University, Beijing. His research interests include digital geometry processing, video processing, rendering, computer animation, and computer-aided geometric design. He is associate editor-in-chief of *The Visual Computer* (Springer), and on the editorial boards of *Computer-Aided Design and Computer & Graphics* (Elsevier). He is a member of the IEEE and ACM.

▷ **For more information on this or any other computing topic, please visit our Digital Library at** www.computer.org/publications/dlib.